Modernizing Thermal Conductivity Equipment for Advanced Jute Material Research

Md. Mahmudul Habib, MA Kaysar, Anas Ali Limon and Zakaria Ahmed*
Technology Wing, Bangladesh Jute Research Institute, Manik Mia Avenue, Dhaka-1207, Bangladesh

Received: Dec 15, 2025
Accepted: Jan 25, 2026
Published: Jan 27, 2026

***Corresponding author:**
Zakaria Ahmed
E-mail: zakaria@bjri.gov.bd

ABSTRACT
Measuring thermal conductivity of a jute-based product is an important aspect to choose the best product to fit for right purpose. For this reason, it is important to measure thermal conductivity with accuracy. In the existing thermal conductivity machine of Physics Department, temperature is measured with analog thermometer. Reading analog thermometer is not precise and accurate enough. Therefore, it is important to measure temperature reading more accurately, that means digitally. Temperature sensor DB18B20, Arduino Nano and a display unit were used to show the temperature digitally. Thermal conductivity of PP, Jute-PP composite, Jute-Polyester composite, and Jute-Wool composite samples was measured both conventionally and digitally. For both conventional and digital approaches, the thermal conductivity values of the samples mentioned above differed by 0.04%, 2.84%, 6.01%, and 5.54%. Considering the heating rate, there is an observable trend: a decrease in specimen width correlates with an increase in heating rate. Additionally, specimens with the same width show varying heating rates depending on the material composition.

KEYWORDS: Thermal conductivity, Arduino Nano, Temperature sensor DB18B20, Resistor, Multimeter, jute

1.INTRODUCTION

Thermal conductivity is one of the important thermophysical properties providing the functional performance and end-use applicability of textile and polymer-based materials. In the context of jute and jute-based composites, thermal conductivity plays a decisive role in determining their suitability for applications such as insulation materials, packaging, automotive interiors, and sustainable construction components. As jute is increasingly promoted as an eco-friendly and renewable alternative to synthetic fibers, accurate characterization of its thermal behavior has become essential for both product development and material selection (Habib et al., 2025). Conventionally, the thermal conductivity of poor conductors such as jute composites is measured using the modified Lee's disc method (Kharshiduzzaman et al., 2019; ASTM D7340-07(2018)e1). Despite its widespread use in academic and industrial laboratories, the conventional Lee's disc apparatus relies heavily on analog thermometers for temperature measurement (Philip and Fagbenle, 2014). This approach introduces significant limitations, including parallax error, limited resolution, operator dependency, and difficulty in continuous data logging (Alazzawi et al., 2024). These factors collectively reduce measurement accuracy and hinder detailed thermal analysis, particularly when transient thermal behavior such as heating and cooling characteristics is of interest.

Recent advances in low-cost microcontrollers and digital temperature sensors have opened new opportunities for modernizing traditional experimental setups (Negreiros et al., 2025). Digital temperature sensors such as the DS18B20 offer high resolution, improved accuracy, and reliable performance over a wide temperature range, while microcontroller platforms like Arduino Nano enable real-time data acquisition, automated calculations, and seamless integration with computer-based data logging systems (Elyounsi and Kalashnikov, 2021). Digitalization of conventional thermal conductivity equipment not only enhances measurement precision but also enables continuous monitoring of temperature evolution, facilitating the construction of heating and cooling curves that are otherwise impractical with analog systems. Beyond steady-state thermal conductivity, the transient thermal response of materials characterized through heating and cooling rates, provides valuable insights into heat storage, dissipation behavior, and thermal inertia (Barragán et al., 2022; Sunday et al., 2012). For composite materials, these properties are strongly influenced by fiber type, matrix material, interfacial bonding, and specimen geometry (Sombatsompop and Wood, 1997). In particular, jute-based hybrid composites exhibit complex thermal behavior due to the combined effects of natural fibers and polymeric constituents (Mohapatra et al., 2014). However, systematic experimental studies that simultaneously evaluate steady-state thermal conductivity and transient heating–cooling behavior of jute-based composites using digitally upgraded instrumentation remain limited.

In this study, a conventional Lee's disc thermal conductivity apparatus was digitally upgraded using DS18B20 temperature sensors, an Arduino Nano microcontroller, and a digital display and data-logging system. The upgraded system enables precise temperature measurement, automated thermal conductivity calculation, and continuous recording of temperature data at fixed time intervals. The thermal conductivity values obtained using the digital system were directly compared with those measured using the conventional analog method to evaluate accuracy, reliability, and deviation between the two approaches. Furthermore, heating and cooling curves were generated for various jute-based materials, including PP sheet, jute-PP composite, jute-polyester composite, and jute-wool composite, allowing comparative analysis of their transient thermal behavior. The outcomes of this work aim to demonstrate the effectiveness of digitalization in improving the accuracy and functionality of traditional thermal conductivity equipment, quantify the differences between conventional and digital measurement techniques, and analyze the influence of material composition and specimen thickness on thermal conductivity, heating rate, and cooling rate of jute-based composites. The findings are expected to contribute to the development of more reliable thermal characterization techniques and support informed material selection for sustainable jute-based applications.

2. MATERIALS AND METHODS

2.1 Materials and Equipment

The existing Lee's disc thermal conductivity apparatus of the Textile Physics Division, Technology Wing, Bangladesh Jute Research Institute (BJRI), was digitally upgraded to improve temperature measurement accuracy and enable automated data acquisition. The upgraded system consisted of both conventional components of the Lee's disc method and additional electronic and digital modules (Fig. 1).

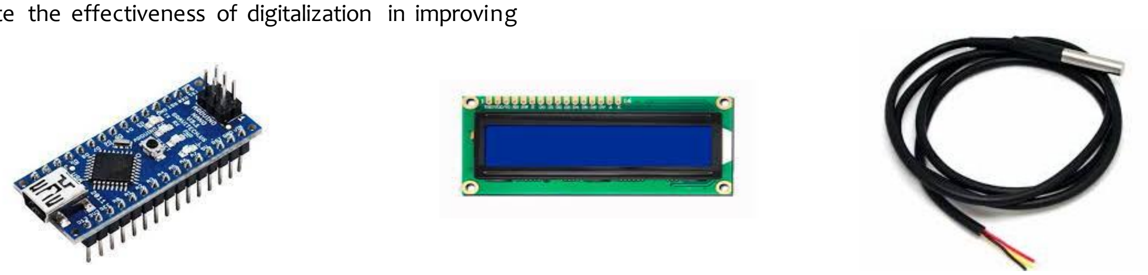

(a) Arduino Uno (b) 16x2 LCD Display (c) DS18B20 Sensor

(d) Matrix Display (e) Multimeter (f) Breadboard

Fig. 1. Required equipment for thermal conductivity machine upgradation

The primary materials and equipment used in this study include:

- Modified Lee's disc thermal conductivity apparatus
- Arduino Nano microcontroller
- DS18B20 digital temperature sensors (three units)
- 16×2 LCD display module
- Push buttons (two units)
- Fixed resistors and connecting wires
- Breadboard and custom-designed printed circuit board (PCB)
- Multimeter for voltage and current measurement
- Regulated DC power supply
- Personal computer with Arduino IDE and Excel

The DS18B20 sensors were selected due to their high accuracy, digital output, and suitability for real-time temperature monitoring over the experimental temperature range.

2.2 Principle of Measurement: Modified Lee's Disc Method

Thermal conductivity measurements were performed using the modified Lee's disc method, which is suitable for poor conductors in the form of flat circular specimens (Fig. 2). In this method, heat flows from an electrically heated upper disc through the test specimen to a lower disc, and steady-state temperatures are established (Sunday et al., 2012; Price and Jarratt, 2002).

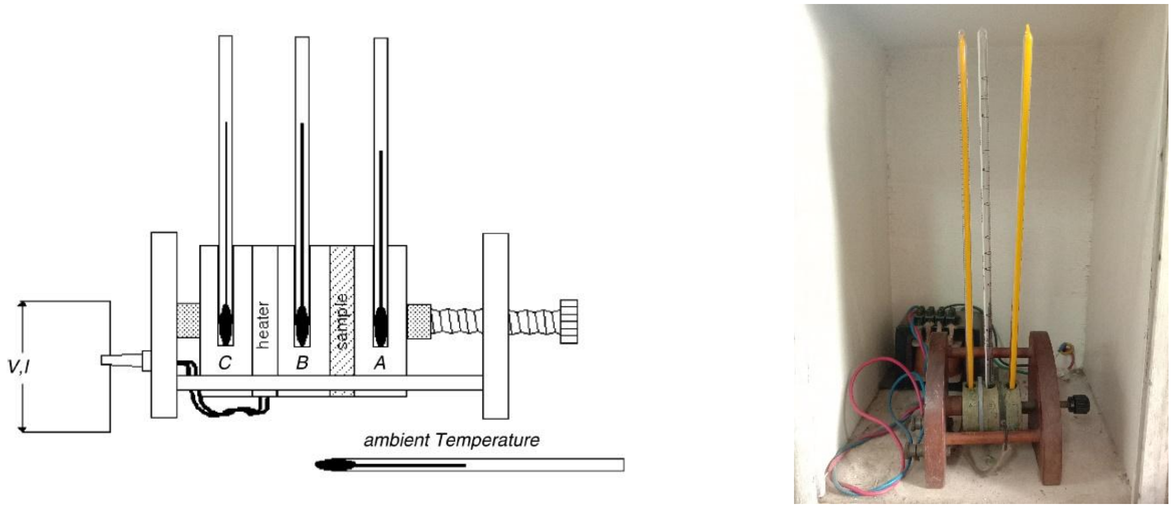

(a) (b)

Figure 2: (a) Schematic diagram of existing thermal conductivity machine and (b) Existing machine setup

Let, *e* joules of energy be emitted from the exposed area of surface (measured in m^2) $s^{-1} {}^{o}C^{-1}$ above ambient temperature. Assume that this is the same for disks A, B, C and the specimen. The temperature of the specimen (T_S) is the mean temperature of disks A and B (Omotoyinbo, et al., 2014) . So, thermal conductivity:

$$K = \frac{ed}{2\pi r^2 \,(T_B - T_A)} \left(2a_A T_A + a_S \frac{T_A + T_B}{2}\right)$$

Where,

e = Amount of heat energy transferred from heat to cold end {Joules/(Sec^{-1} m^{-2} °C^{-1})}

d= Thickness of sample (m)

L = Width of material in machine = 12.7 ×10^{-3} m

l = Width of heater in machine = 4.8 ×10^{-3} m

r = radius of circular copper disc = 2.06×10^{-2} m^2

T_A = Temperature of Disc A (°C)

T_B = Temperature of Disc B (°C)

T_C = Temperature of Disc C (°C)

a_A= Surface area of Disc A = $a_A = \pi r^2 + 2\pi r d$ = 29.755×10^{-4} m^2

a_B= Surface area of Disc B = $a_B = 2\pi r L$ =16.430×10^{-4} m^2

a_C= Surface area of Disc C = $a_C = \pi r^2 + 2\pi r L$ =29.755×10^{-4} m^2

a_S= Surface area of Sample = $2\pi r d$ m^2

a_H= Surface area of Heater = $2\pi r l$ = 6.21×10^{-4} m^2

V = One of the potential differences across element in volt = 6.4 volt

I = The current flowing in ampere = 0.35 ampere

W = VI = 2.24 Joules/Sec = 2.24 watts

2.3 Digitalization of the Thermal Conductivity Apparatus

To overcome the limitations of analog thermometry, three DS18B20 digital temperature sensors were integrated into the apparatus. The sensors were placed in thermal contact with disc A, disc B, and disc C, respectively. These sensors were interfaced with an Arduino Nano microcontroller, which served as the central processing and control unit. The Arduino Nano performed the following functions:

- Real-time temperature acquisition from all sensors
- Automated detection of steady-state temperature conditions
- Calculation of thermal conductivity using programmed equations
- Display of temperature and thermal conductivity values on an LCD screen
- Storage and transfer of temperature data for further analysis

Temperature data were recorded at 10-second intervals and saved in spreadsheet format for subsequent plotting of heating and cooling curves.

2.4 Programming and Control Algorithm

The control and data acquisition program were developed using the Arduino IDE. The algorithm followed the steps below:

- Measurement of specimen diameter and thickness and manual input through the keypad
- Continuous temperature measurement using three DS18B20 sensors
- Storage of temperature values in Arduino EEPROM
- Comparison of temperature values at 5-minute intervals
- Verification of steady-state condition (temperature variation ≤ 0.5 °C per 5 minutes)
- Automatic execution of thermal conductivity calculation
- Display of calculated thermal conductivity on the LCD
- Logging of temperature data at 10-second intervals
- Generation of heating and cooling curves from recorded data
- Determination of heating and cooling rates from curve slopes

This automated process minimized operator intervention and ensured consistent measurement conditions across all experiments.

2.5 Hardware Design and Circuit Integration

Initially, the circuit layout was designed on paper and tested using a breadboard to verify functionality and identify potential errors (Fig 3, 4. 5). After successful testing, the final circuit was designed using Fritzing software and fabricated on a copper-clad PCB with protective masking.

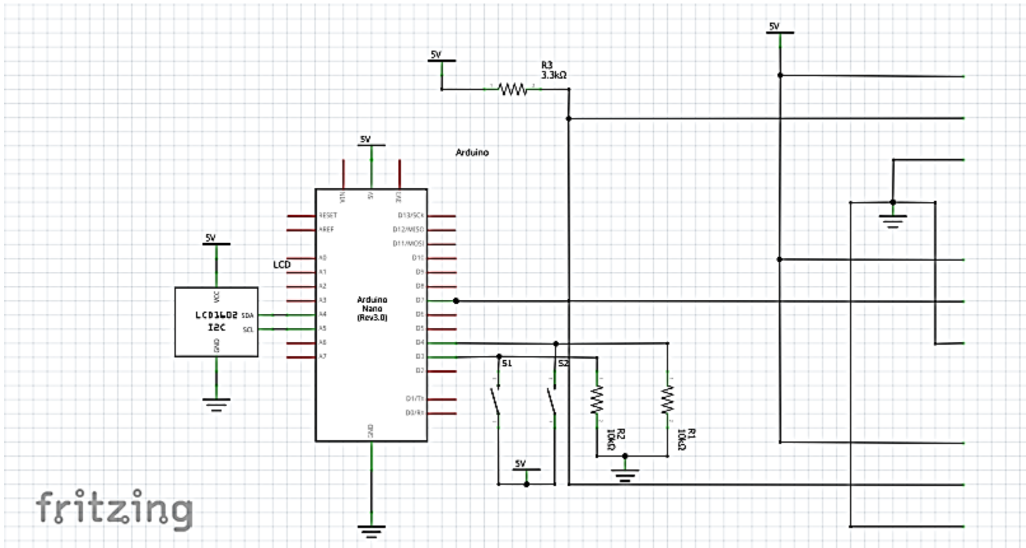

Fig. 3. Schematic diagram of circuit connection of digital thermal conductivity machine

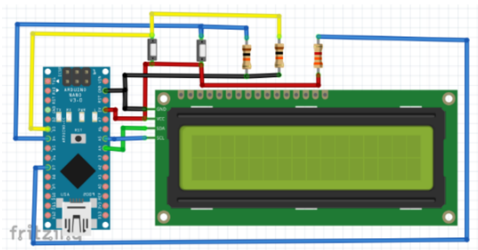

Figure 4: Breadboard diagram of circuit connection of digitalized part of thermal conductivity machine

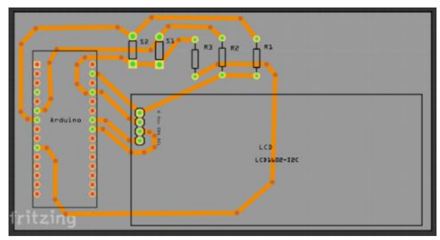

Figure 5: PCB diagram of circuit connection of digitalized part of thermal conductivity machine

(a) LCD Display

(b) Push Button

(c) DS18B20 Temperature sensors

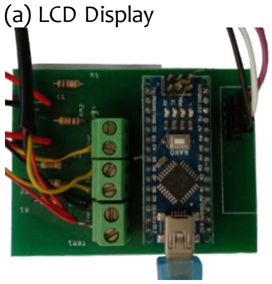

(d) Designed PCB Board front side

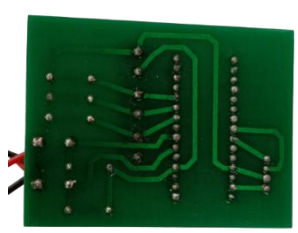

(e) Designed PCB Board back side

Fig. 6. Different parts of digital thermal conductivity machine

All electronic components were soldered onto the PCB following the finalized layout (Fig. 6). After hardware assembly, the Arduino Nano was programmed and interfaced with the system via a USB connection to the computer.

2.6 Specimen Preparation

Four types of materials were selected for this study:

- Polypropylene (PP) sheet
- Jute–PP composite
- Jute–polyester composite
- Jute–wool composite

All specimens were prepared in circular disc form to match the dimensions of the Lee's disc apparatus. The discs had a diameter of 41.2 mm, while specimen thickness varied depending on material type (Fig. 7). Thickness was measured using a digital micrometer prior to testing. Each specimen was conditioned at ambient laboratory conditions before testing to ensure thermal equilibrium.

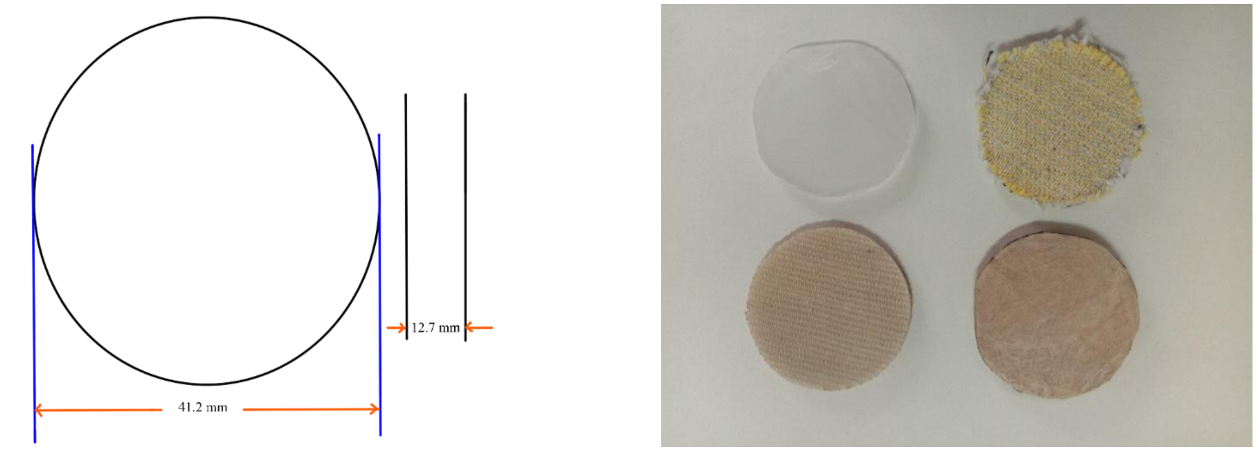

(a) (b)

Fig. 7. (a) Disk dimension radius: 41.2 mm, width: 12.7 mm (b) Prepared specimens

2.7 Experimental Procedure

For each specimen, thermal conductivity was measured using both the conventional analog method and the digitally upgraded system. In the digital method, the apparatus was allowed to reach steady-state conditions before thermal conductivity values were recorded. Temperature-time data were continuously logged during both heating and natural cooling phases. Heating and cooling curves were plotted using OriginPro software, and the corresponding heating and cooling rates were calculated from the slopes of the curves. All measurements were repeated to ensure consistency and reliability of the results.

3. RESULTS AND DISCUSSION

3.1 Comparison of Thermal Conductivity Measured by Conventional and Digital Methods

The thermal conductivity values of PP sheet, jute-PP composite, jute-polyester composite, and jute-wool composite measured using both conventional analog and digitally upgraded Lee's disc methods are presented (Table 1). The results demonstrate that the digital system yields values closely comparable to those obtained by the traditional method, with percentage deviations ranging from 0.04% to 6.01%.

Table 1. Values of thermal conductivity by conventional and digital method

Parameters	Jute-PP Composite	Jute-Polyester Composite	PP Sheet	Jute-wool Composite
TC (Digital) ($Wm^{-1}K^{-1}$)	0.2905686	0.274948	0.3164666	0.2407086
TC (Conventional) ($Wm^{-1}K^{-1}$)	0.299071026	0.259358076	0.316352158	0.228082711
Difference	0.008502426	0.015589924	0.000114442	0.012625889
Difference (%)	2.84%	6.01%	0.04%	5.54%

Among the tested materials, the PP sheet exhibited the smallest deviation (0.04%) between the two methods, indicating excellent agreement. This can be attributed to the relatively homogeneous and isotropic nature of PP, which leads to stable heat flow and reduced sensitivity to small temperature measurement errors. In contrast, the jute–polyester composite showed the highest deviation (6.01%), followed by jute-wool (5.54%) and jute-PP composites (2.84%). These higher deviations are primarily associated with the heterogeneous structure of natural fiber composites, where fiber distribution, interfacial thermal resistance, and porosity can significantly influence temperature gradients across the specimen.

3.2 Heating Curve Analysis and Effect of Specimen Thickness

The heating curves of the four specimens with different thicknesses are shown below (Fig. 8). The slopes of these curves were used to calculate heating rates (Table 2). A clear inverse relationship between specimen thickness and heating rate is observed, thinner specimens heat up more rapidly than thicker ones.

Table 2. Heating rates for the PP sheet, Jute-PP composite, Jute-Polyester composite, and Jute-Wool composite

Sample Name	Width	Thermal Conductivity ($Wm^{-1}K^{-1}$)	Heating Rate
PP sheet	3.40	0.3164666	0.34648
Jute-PP composite	5.76	0.2905686	0.28904
Jute-Polyester composite	2.88	0.274948	0.37938
Jute-Wool composite	1.73	0.2407086	0.38714

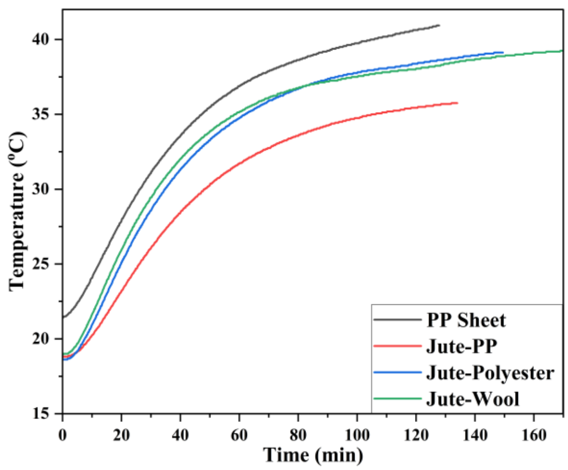

Figure 8. Heating curve of PP sheet, Jute-PP composite, Jute-Polyester composite, and Jute-Wool composite specimens of different width

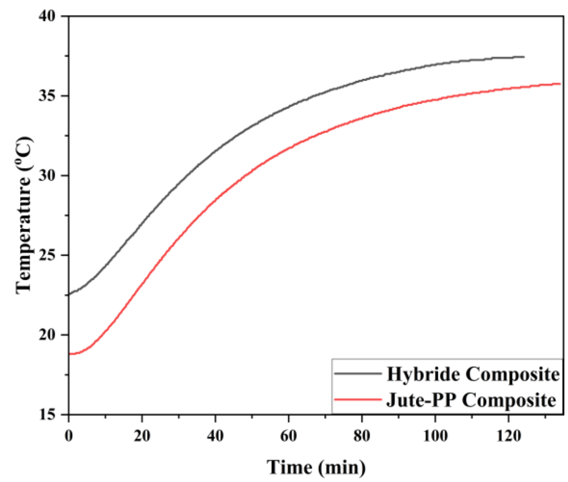

Figure 9. Heating curve of Hybrid and Jute-PP composite of same width

This behavior is consistent with classical heat transfer theory, where reduced thickness lowers thermal resistance and facilitates faster temperature rise under identical heat input. The jute-wool composite, which had the smallest thickness, exhibited the highest heating rate, while the jute–PP composite, with the largest thickness, showed the lowest heating rate.

Comparable trends have been reported for natural fiber reinforced polymer composites, where thinner samples exhibit higher heating rates due to reduced heat diffusion paths (Dev et al., 2023). Additionally, the porous structure of jute fibers contributes to air entrapment, which acts as a thermal barrier and modifies transient heat flow behavior.

3.3 Influence of Material Composition at Constant Thickness

To isolate the effect of material composition, heating rates of hybrid composite and jute-PP composite specimens with identical thickness (5.76 mm) were compared (Table 3 and Fig. 9). Despite having the same thickness, the jute-PP composite exhibited a higher heating rate than the hybrid composite.

Table 3. Heating rates for the Hybrid composite, Jute-PP composite

Sample Name	Width	Heating Rate
Hybrid Composite	5.76	0.25225
Jute-PP composite	5.76	0.28904

This difference can be explained by the higher thermal conductivity of polypropylene compared to other reinforcing or matrix constituents present in the hybrid composite. The polymer-rich structure of the jute-PP composite facilitates faster heat transfer, whereas the hybrid composite likely contains interfaces and fiber combinations that increase interfacial thermal resistance. Similar composition-dependent variations have been observed in studies on jute-polyester and jute-epoxy composites, where thermal conductivity and heating behavior strongly depend on matrix type, fiber volume fraction, and interfacial bonding (Alazzawi et al., 2024). These findings emphasize that thickness alone cannot fully explain thermal behavior; material composition plays a decisive role.

3.4 Heating and Cooling Curve Characteristics

Figure 10 presents the heating and cooling curves for selected jute-PP and jute-polyester composite specimens. The corresponding heating and cooling rates are listed in Table 4. For all samples, the heating rate was consistently higher than the cooling rate.

Table 4. Heating and cooling rates for the Jute-Polyester composite, Jute-PP composite having different width

Sample Name	Heating Rate (°C/min)	Cooling Rate (°C/min)
Jute-PP composite (5.38mm)	0.26982	0.20774
Jute-Polyester composite (2.98mm)	0.30545	0.26067
Jute-Polyester composite (3.38mm)	0.29889	0.25534

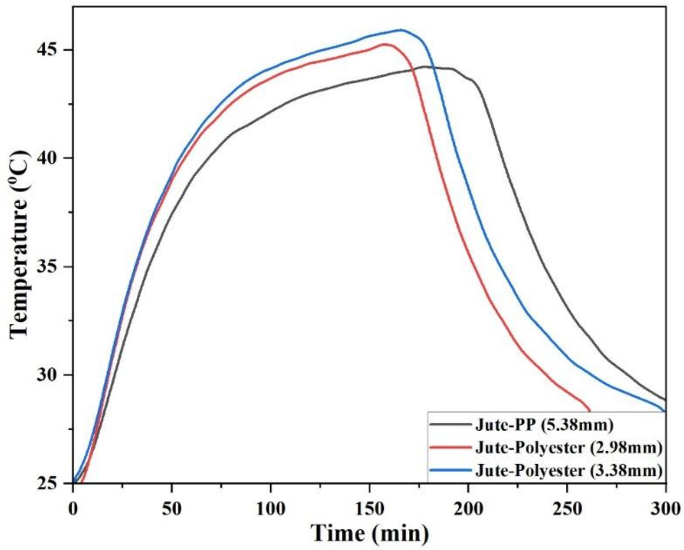

Fig. 10. Heating and cooling curve of Jute-Polyester and Jute-PP composite of same width

This asymmetry between heating and cooling behavior is characteristic of materials with finite heat storage capacity and thermal inertia. During heating, continuous electrical power input drives temperature rise, whereas cooling occurs through natural convection and radiation, which are comparatively slower processes. Similar heating-cooling asymmetry has been reported in thermal characterization studies of polymeric and natural fiber composites using transient methods. Furthermore, for specimens of the same material, both heating and cooling rates decreased with increasing thickness. This trend reinforces the role of specimen geometry in governing transient heat transfer and aligns well with Fourier's law and lumped thermal mass models used for poor conductors.

3.5 Implications for Jute-Based Material Selection

The combined analysis of steady-state thermal conductivity and transient heating-cooling behavior provides a more comprehensive understanding of thermal performance than thermal conductivity alone. While PP sheets exhibited the highest thermal conductivity, jute-based composites demonstrated comparatively lower values, making them more suitable for insulation-related applications. Among the composites, jute-wool showed higher heating rates but lower thermal conductivity, suggesting faster thermal response with improved insulation potential. These characteristics are particularly relevant for applications such as thermal liners, packaging, and eco-friendly building materials, where controlled heat transfer is desirable. The ability of the digitalized system to simultaneously capture steady-state and transient thermal data represents a significant advancement over conventional setups and aligns with modern experimental practices in thermal materials research.

4. CONCLUSIONS

In this work, an existing Lee's disc thermal conductivity apparatus was upgraded by introducing digital temperature sensing and microcontroller-based data processing. The use of DS18B20 sensors and an Arduino Nano allowed temperature to be measured more precisely and consistently than with the traditional analog thermometers, while also enabling automatic data recording and calculation. The thermal conductivity values obtained from the digital system were found to be in close agreement with those measured by the conventional method. The difference between the two approaches remained small, particularly for the PP sheet, whereas slightly larger deviations were observed for jute-based composites. This behavior is likely related to the non-uniform and heterogeneous nature of natural fiber composites, where small temperature variations can have a noticeable effect on calculated values. Overall, the results indicate that the digital system provides reliable measurements with improved repeatability. An important advantage of the digitalized setup is the ability to analyze transient thermal behavior. The heating and cooling curve analysis showed that thinner specimens heat and cool faster than thicker ones, and that materials of the same thickness can still behave differently depending on their composition. These observations are consistent with basic heat transfer principles and highlight the influence of both geometry and material structure on thermal response. The results further suggest that jute-based composites have lower thermal conductivity than PP, supporting their potential use in applications where thermal insulation is required. By combining steady-state thermal conductivity measurement with heating and cooling analysis, this study provides a more complete picture of the thermal performance of jute-based materials. Overall, the digitalization of the Lee's disc apparatus has improved both the accuracy and usefulness of the experiment, while keeping the system simple and low-cost. The upgraded setup can be readily adopted in research laboratories and teaching environments for the thermal characterization of natural fiber composites and similar materials.

5. REFERENCES

Alazzawi S, Mahmood WA and Shihab SK (2024) Comparative Study of Natural Fiber-Reinforced Composites for Sustainable Thermal Insulation in Construction. International Journal of Thermofluids. 24. DOI: 100839. 10.1016/j.ijft.2024.100839.

ASTM D7340-07(2018)e1 (2023) Standard Practice for Thermal

Conductivity of Leather Effective Date: 01-Dec-2023.

Barragán VM, Maroto JC, Pastuschuk E and Muñoz S (2022) Testing a simple Lee's disc method for estimating throuh-plane thermal conductivity of polymeric ion-exchange membranes. Int. J. Heat Mass Transf. 184: 122295.

Dev B, Rahman MA, Repon MR, Rahman MM, Haji A and Nawab Y (2023) Recent progress in thermal and acoustic properties of natural fiber reinforced polymer composites: Preparation, characterization, and data analysis. Polymer. Composite. 44(11): 7235–7297.

Elyounsi A and Kalashnikov AN (2021) Evaluating Suitability of a DS18B20 Temperature Sensor for Use in an Accurate Air Temperature Distribution Measurement Network. Engineering Proceedings. 10: 56. DOI: 10.3390/ecsa-8-11277.

Habib A, Islam MA, Hossain MT *et al.* (2025) Recent developments in the modification and fabrication of jute fibre-reinforced composites for structural applications. Discover Sustainability. 6(1): 1107. DOI: https://doi.org/10.1007/s43621-025-01785-7.

Kharshiduzzaman M, Hossain MS, Ali S and Ahmed S (2019) Determination of the thermal conductivity of poor conductive materials in the form of disc by self-constructed Lee's disc apparatus. AIP Conference Proceedings. 2121. DOI: 140008. 10.1063/1.5115959.

Mohapatra RC, Mishra A and Choudhury BB (2014) Measurement on Thermal Conductivity of Pine Wood Dust Filled Epoxy Composites. American Journal of Mechanical Engineering. 2(4): 114–119.

Negreiros WJA, Rodrigues G, Ribeiro JDS, Silva MM, Junio DS, Seruffo RFP, Monteiro SN and Corrêa ADC (2025) Development and Validation of a Low-Cost Arduino-Based Lee Disc System for Thermal Conductivity Analysis of Sustainable Roofing Materials. Sensors. 25(17): 5447. DOI: https://doi.org/10.3390/s25175447

Omotoyinbo, JA, Oladele I and Shokoya W (2014) Effect of the Degree of Plastic Deformation on the Electrical Resistance and Thermal Conductivity of Al-Mg-Si Alloy. Leonardo Electronic Journal of Practices and Technologies. 13: 37-50.

Price DM and Jarratt M (2002) Thermal conductivity of PTFE and PTFE composites. Thermochimica Acta. 392–393:231–236. DOI: https://doi.org/10.1016/S0040-6031(02)00105-3.

Philip P and Fagbenle L (2014) Design of lee's disc electrical method for determining thermal conductivity of a poor conductor in the form of a flat disc. International Journal of Innovation and Scientific Research. 9(2): 335–343. DOI: https://ijisr.issr-journals.org/abstract.php?article=IJISR-14-221-01.

Sunday SO, Olawale RB and Olabode JY (2012) Thermal Conductivity of Three Different Wood Products of Combretaceae Family. Journal of Natural Sciences Research, 2(9): 18-29.

Sombatsompop N and Wood AK (1997) Measurement of thermal conductivity of polymers using an improved Lee's Disc apparatus. Polymer Testing, 16(3): 203–223.

Author Contributions
All the authors conceived the concept, wrote and approved the manuscript.

Acknowledgements
Not applicable.

Funding
Not applicable.

Availability of data and materials
Not applicable.

Competing interest
The authors declare no competing interests.

Ethics approval
Not applicable.

Citation: Md. Mahmudul Habib, MA Kaysar, Anas Ali Limon and Zakaria Ahmed (2026) Modernizing Thermal Conductivity Equipment for Advanced Jute Material Research. Technol TIMES 1(1): 1-8.